Interference Effects in the Multiphoton Ionization of Sodium

R. R. Jones
Department of Physics, University of Virginia, Charlottesville, Virginia 22901
(Received 23 August 1994)

Sodium atoms are ionized by 777 nm, 150 fs laser pulses. Modulations are observed in the multiphoton ionization yield as a function of laser intensity. The oscillations are attributed to Ramsey interference caused by coherent population transfer between bound states at two different times during a single laser pulse.

PACS numbers: 32.80.Rm, 32.80.Wr

The study of atoms in intense electromagnetic fields has been a topic of great interest for many years due to the nonperturbative nature of the interaction [1]. The extremely high fields which are available in current laser pulses makes them extremely attractive for this type of research. Unfortunately, typical focused laser experiments are plagued by spatial intensity variation which can mask important intensity-dependent coherence effects.

This Letter describes an experiment where an unfocused laser beam is used to study multiphoton ionization in Na. Ramsey [2] or Stueckelberg [3] oscillations are observed in the ionization signal as a function of laser intensity. These modulations are produced by interference in the excitation of bound states which are subsequently ionized [4]. The interference occurs due to the interaction of two or more bound states at two different points in time during a single laser pulse. The modulations have been obscured in all previous experiments due to spatial intensity variations in focus laser beams. They are observed here for the first time using an unfocused beam geometry.

The mechanism responsible for the interference observed in this experiment is very general in nature. Consider a system of two levels which are coupled together during two temporally separated time intervals. Assume the probability for finding the atom in state 1 is equal to unity at $t = -\infty$. During the first interaction period, some population is transferred to state 2. If the two interactions are temporally coherent, then the probability for finding the atom in state 2 after the second interaction depends on the sine of the relative phase $\Delta\Phi$ between the two states (in units of a.u.)

$$\Delta\Phi = \int_{\tau_1}^{\tau_2} [E_1(t) - E_2(t)]\,dt + \phi_0, \qquad (1)$$

where τ_1 and τ_2 are the two interaction times, $E_{1,2}(t)$ are the time-dependent energies of the two levels, and ϕ_0 depends on the strength and nature of the interaction. If more than two states are involved, then the probability for finding population in any level is a complicated function of the relative phases between all interacting states [5].

In the experiment, a single laser pulse is used to ionize ground state Na atoms. During the ionization process, population is transferred to excited states via ac Stark shifted resonances which occur twice during the pulse—once as the laser pulse "turns-on" and again as the pulse "turns-off" [4]. As the peak laser intensity is increased, the interval between the interaction times τ_1 and τ_2 increases, and the maximum energy shifts of the bound states change. In fact, for each pair of interacting levels, $\Delta\Phi$ increases with increasing intensity, causing modulations in the excited state population. Since most of the ionization occurs via single-photon absorption out of these high lying states, oscillations are observed in the total ionization yield as well. Modulations in excited state population [6] and total ionization yield [7,8] as a function of the intensity of a single electromagnetic pulse have been predicted theoretically. Furthermore, Stueckelberg oscillations [3] in the transfer of population between bound states have been observed in microwave experiments [9]. However, until now these effects have gone undetected in laser experiments.

Figure 1(a) shows an energy level diagram for the Na atom as a function of laser intensity. The energies are plotted relative to the ground state. In the presence of low intensity 777 nm radiation, the ground state of Na is in two-photon resonance with the $4s$ excited level and only 70 cm^{-1} off of three-photon resonance with the $7p$ state. As the laser pulse turns-on, the $4s$ level shifts out of resonance, and the $7p$ state shifts into resonance. Depending on the peak intensity in the pulse, the ground state will come into three-photon resonance with several other excited states ($6f$, $6p$, $5f$, etc.) at different times during the "turn-on" of the laser pulse. These resonances occur again as the pulse turns off. In a "dressed state" or Floquet description [10], the intensity-dependent resonances appear as avoided level crossings as shown in Fig. 1(b). Figures 1(a) and 1(b) are obtained by diagonalizing a Floquet Hamiltonian matrix. The matrix includes nine field free states ($3s$, $3p$, $4s$, $3d$, $4p$, $6p$, $5f$, $7p$, and $6f$) and six additional Floquet blocks [10] corresponding to the field free states ± 1, ± 2, and ± 3 photons. Since no continuum states are included, the eigenvalues are all real. The lack of continuum coupling should not significantly affect the dressed state energies except possibly near avoided crossings. The off-diagonal matrix elements are calculated in the "velocity" gauge [7] using the dipole approximation and a Numerov integration routine [11].

0031-9007/95/74(7)/1091(4)$06.00

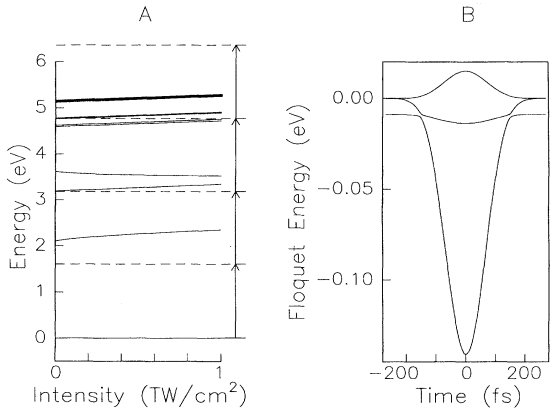

FIG. 1. (a) Energy levels in Na as a function of laser intensity. The discrete energy levels are shown in order of increasing energy: $3s$, $3p$, $4s$, $3d$, $5f$, $6p$, $6f$, and $7p$. The length of the arrows corresponds to the photon energy. The bold line denotes the ionization threshold. (b) Energies of three "dressed" states as a function of time during a 150 fs laser pulse for a peak intensity of 1.0 TW/cm^2. At low intensity the dressed states can be labeled from top to bottom as $|4s - 2\omega\rangle$, $|3s\rangle$, and $|7p - 3\omega\rangle$. The modulation in the ionization signal with increasing intensity is due primarily to the avoided crossing traversals between the dressed ground state and $7p$ level during the rising and falling edges of the laser pulse.

The 150 fs, 777 nm laser pulses used in the experiment are generated using chirped-pulse amplification of a train of pulses from a self-mode-locked Ti:sapphire oscillator. The amplifier system consists of a grating pulse expander, a regenerative preamplifier, a three-pass power amplifier, and a grating pulse compressor. The energy of the laser pulse is varied by rotating a half-wave plate before the pulse compressor which acts as a 30:1 polarizer. The maximum pulse energy used in the experiments is 20 mJ, yielding a peak power of >0.1 TW per pulse.

The laser pulse crosses a thermal beam of ground state Na atoms at right angles in a vacuum chamber with a background pressure of 10^{-6} Torr. The laser and atomic beams intersect between two parallel capacitor plates that are separated by 1.5 cm. A static voltage (20–300 V) produces a small electric field between the plates. Any ions which are formed by the laser pulse are accelerated by the dc field through a 1 mm hole in the upper plate.

A 250 mm focal length lens reduces the 7 mm diameter (FWHM) laser beam to a diameter of >3 mm (FWHM) in the interaction region [12]. The beam is actually diverging beneath the extraction hole, but the variation in the laser intensity over the 1 mm hole diameter is negligible. Because the extraction aperture is significantly smaller than the laser beam diameter, any detected ions which are created at a particular vertical location between the capacitor plates experience the same peak intensity. Ions originating at different vertical positions experience different peak intensities due to the spatial variation of the laser beam along the vertical dimension.

The small extraction field allows ions which are born at different vertical positions to be distinguished from each other. Upon leaving the region between the capacitor plates, each ion acquires a kinetic energy equal to its potential energy at the instant of its creation. Thus, ions born at different vertical positions acquire different kinetic energies and arrive at the microchannel plate detector at different times. Ions which experience the maximum available intensity as well as those created far in the wings of the spatial intensity profile can be detected and distinguished in a single laser shot.

Figure 2 shows a series of time-of-flight (TOF) ion spectra taken at several different pulse energies. Each oscilloscope trace shows a broad TOF peak which exhibits clear modulations. The number of oscillations in the spectra is dependent on the energy in the laser pulse. No oscillations are observed at low energies, and several modulations can be seen in the highest energy trace. With decreasing intensity, the modulations near the center of the profile disappear as those near the wings move toward the center. Each spectrum shows the ionization probability at all intensities between the pulse maximum and zero. The modulations indicate structure in the ionization probability over the smoothly varying spatial intensity envelope.

The ionization signal from different locations within the laser spatial profile can be simultaneously recorded as a function of pulse energy. Up to 12 time bins are used to sample the ionization signal in narrow bands across the TOF spectrum. Bins positioned in the center of the TOF spectrum measure the ionization signal from

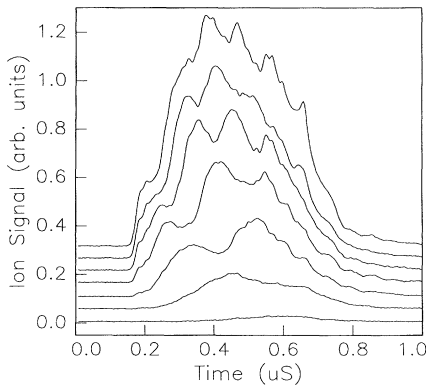

FIG. 2. Ionization signal vs time for several different laser pulse energies. The ion spectrometer converts vertical position in the laser intensity profile to flight time to the detector. The modulations in the broad TOF spectra are due to the intensity dependence of the ionization probability within the smooth intensity distribution of the pulse. From top to bottom the traces correspond to peak intensities of 1.0, 0.89, 0.77, 0.60, 0.45, 0.29, and 0.15 TW/cm^2. The traces have been vertically offset from each other to avoid overlapping lines. The zero of the time scale is several microseconds after the laser-atom interaction time.

the region of maximum laser intensity. Figure 3 shows the ionization spectrum recorded in six different time bins. The peak intensity in the laser is 1.0 TW/cm^2 for a 20 mJ pulse. The ionization signal displayed in the upper light trace corresponds to the center of the "focal" volume (i.e., the peak laser intensity), while that in the lower traces corresponds to the wings of the intensity distribution. Each trace in Fig. 3 has been normalized separately. A clear modulation is evident in all curves, but the oscillation frequency and phase are different for each. Note that the ionization signal can actually *decrease* with increasing laser intensity. Integration of the ion signal over the entire interaction volume causes complete cancellation of the oscillations as can be seen in the bold trace at the top of the figure.

The modulations in the ionization probability are caused by Ramsey [2] or Stueckelberg [3] interference which occurs in the excitation of bound states during the rising and falling edges of the laser pulse. Since the total ionization yield is dominated by single-photon absorption out of these states, the modulations in the excited state population are reflected in the ionization signal. A complete oscillation in the transition probability between two bound states occurs when the phase difference, $\Delta\Phi$, changes by 2π [see Eq. (1)]. In this experiment, interfering transitions between the $7p$ level and the ground state "dressed" by three photons [see Fig. 1(b)] are the primary source of the modulations. For a given peak intensity, the integral in Eq. (1) can be determined by computing the area between the energy curves for these two states [see Fig. 1(b)]. This geometric approach predicts a relative phase difference between the dressed ground state and the $7p$ level of $\Delta\Phi = 9.25\pi$ for a 150 fs pulse with a peak intensity of 1.0 TW/cm^2. Therefore, one would expect to see 4.6 fringes in the ionization signal during an intensity scan from 0 to 1 TW/cm^2, in good agreement with the experiment (see the upper light trace in Fig. 3).

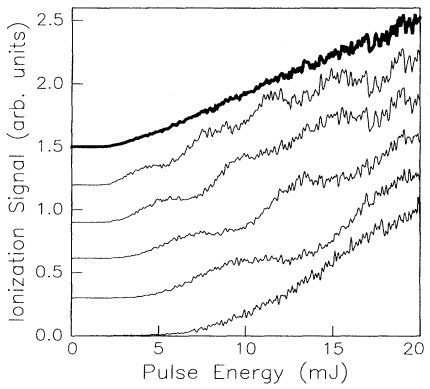

FIG. 3. Ionization signal from six different time bins within the TOF ion signal (see Fig. 2) as a function of pulse energy. The upper light trace shows ions created at the position of highest intensity (up to 1 TW/cm^2), and the lower-most trace is due to ions produced in the spatial intensity wings. Each trace has been individually normalized to unity and offset from zero for clarity. Clear modulations can be seen in all of the scans. The frequency of the oscillations is dependent on intensity, and, therefore, on where the ions are created within the focal volume. The bold curve at the top of the figure is the ionization signal integrated over the entire spatial intensity distribution. Note that no modulations are visible in this trace.

Although the description in the preceding paragraph predicts the correct oscillation period, it does not given any indication as to the modulation depth or contrast. The relative amplitude of the oscillations compared to the total ionization yield depends on the ionization rate out of the populated states between the two resonance times as well as off-resonant transitions which can occur at any time during the pulse. Furthermore, interferences between the dressed ground state and excited levels other than $7p$ may occur during the pulse. The details of the ionization process are dependent on the couplings between the dressed states, the slew rate of the laser intensity at the avoided crossings, and the ionization probability out of each state.

In order to treat the problem more quantitatively, the time-dependent Schrödinger equation is numerically integrated using nine bound states ($3s$, $3p$, $3d$, $4s$, $4p$, $5f$, $6p$, $6f$, and $7p$) and an effective continuum. Ionization out of the four highest energy states is simulated by leaking population out of each level at a rate equal to the single-photon ionization rate at that instant during the pulse. At the end of the pulse, the total photoionization probability is taken as the difference in the total bound state population from unity. The calculation is performed in the velocity gauge [7] using the rotating wave and dipole approximations. The off-diagonal matrix elements are calculated using the bound state energies and Numerov integration [11]. The single-photon ionization rates are obtained using hydrogenic bound and continuum wave functions.

The results of the calculation shown in Fig. 4 assume the same pulse energy and beam diameter as in the experiment. However, the pulse duration which gives the best overall agreement with the data (compare with the uppermost light trace in Fig. 3) is 175 rather than 150 fs. The predicted modulations occur at the same locations as those observed in the experiment. In addition, the relative amplitude of the oscillations compared to the total ionization yield is very similar to that seen experimentally.

Close inspection of Figs. 3 and 4 indicates that the general shapes of the experimental and theoretical ionization curves are not in perfect agreement. Although the form of the theoretical curve is fairly insensitive to small changes in the numerical parameters, possible sources for the observed discrepancies include (1) the limited basis set used for the calculations, in particular, the absence of any true continuum levels; (2) small uncertainties in the matrix elements and photoionization rates; (3) uncertainties in the precise experimental pulse shape, duration, and frequency; and (4) residual spatial averaging in the data collection.

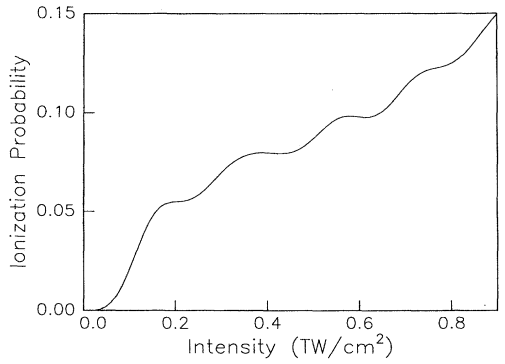

FIG. 4. Calculated ionization probability as a function of intensity for a 175 fs, 777 nm laser pulse. This curve should be compared to the upper light trace in Fig. 3. The predicted modulation depth and fringe spacing are in good agreement with the experimental data.

In summary, time-domain Ramsey interference has been observed in laser-driven multiphoton ionization for the first time. ac Stark shifted resonances which occur twice in a single laser pulse generate modulations in the ionization yield as a function of laser intensity. The experimental observations are in good agreement with a simple physical picture as well as numerical simulations. In addition, the results demonstrate the importance of transient bound-state resonances and atom-laser phase coherence in the multiphoton ionization process. Future experiments may be aimed at exploiting these coherences to control population transfer and ionization in atoms.

It is a pleasure to acknowledge helpful conversations with T. F. Gallagher, J. G. Story, and P. H. Bucksbaum. This work has been supported by the Office of Naval Research.

[1] G. Mainfray and C. Manus, Rep. Prog. Phys. **54**, 1333 (1991); A. L'Huillier, K. J. Schafer, and K. C. Kulander, J. Phys. B **24**, 3315 (1991); R. R. Freeman and P. H. Bucksbaum, *ibid.* **24**, 325 (1991); K. Burnett, V. C. Reed, and P. L. Knight, *ibid.* **26**, 561 (1993).

[2] N. F. Ramsey, *Molecular Beams* (Oxford Univ. Press, New York, 1956).

[3] E. C. G. Stueckelberg, Helv. Phys. Acta **5**, 369 (1932).

[4] R. R. Freeman, P. H. Bucksbaum, H. Milchberg, S. Darack, D. Schumacher, and M. E. Geusic, Phys. Rev. Lett. **59**, 1092 (1987); T. J. McIlrath, R. R. Freeman, W. E. Cooke, and L. D. van Woerkom, Phys. Rev. A **40**, 2770 (1989); M. P. de Boer and H. G. Muller, Phys. Rev. Lett. **68**, 2747 (1992); R. R. Jones, D. W. Schumacher, and P. H. Bucksbaum, Phys. Rev. A **47**, R49 (1993); J. G. Story, D. I. Duncan, and T. F. Gallager, Phys. Rev. Lett. **70**, 3012 (1993); R. B. Vrijen, J. H. Hoogenraad, H. G. Muller, and L. D. Noordam, *ibid.* **70**, 3016 (1993).

[5] R. R. Jones, C. S. Raman, D. W. Schumacher, and P. H. Bucksbaum, Phys. Rev. Lett. **71**, 2575 (1993).

[6] H. P. Breuer, K. Dietz, and M. Holthaus, Z. Phys. D **10**, 13 (1988).

[7] M. Dorr, R. M. Potvliege, and R. Shakeshaft, J. Opt. Soc. Am. B **7**, 433 (1990).

[8] X. Tang, A. Lyras, and P. Lambropoulos, J. Opt. Soc. Am. B **7**, 456 (1990); G. Gibson, R. R. Freeman, T. J. McIlrath, and H. G. Muller, Phys. Rev. A **49**, 3870 (1994).

[9] M. C. Baruch and T. F. Gallagher, Phys. Rev. Lett. **68**, 3515 (1992); S. Yoakum, L. Sirko, and P. M. Koch, *ibid.* **69**, 1919 (1992).

[10] J. H. Shirley, Phys. Rev. **138**, B979 (1965).

[11] M. L. Zimmerman, M. G. Littman, M. M. Kash, and D. Kleppner, Phys. Rev. A **20**, 2251 (1979).

[12] Moving the position of the lens with respect to the interaction region changes the diameter of the beam, and, therefore, the intensity of the pulse beneath the extraction hole. This method for changing the pulse intensity is used to cross-check results obtained by varying the pulse fluence with the half-wave plate.